Preprints of the 21st IFAC World Congress (Virtual)
Berlin, Germany, July 12-17, 2020

Frequency Response Data-based Disturbance Observer Design via Convex Optimization ⋆

Xiaoke Wang, Wataru Ohnishi, Takafumi Koseki *

* *The University of Tokyo, Tokyo, Japan, (e-mail: wangxiaoke@koseki.t.u-tokyo.ac.jp, ohnishi@ieee.org, takafumikoseki@ieee.org)*

Abstract: To estimate and compensate disturbances effectively, disturbance observer (DOB) has been widely employed in industrial field. This paper is dedicated to designing DOB by directly utilizing frequency response data. By transforming all the non-convex constraints into convex form, the bandwidth of DOB is maximized through iterative convex optimization process. Simulation results have verified the effectiveness of the proposed method.

Keywords: Disturbance observer, frequency response data, bandwidth maximization, convex optimization

1. INTRODUCTION

Unavoidable disturbances deteriorate the performance of industrial control systems, especially in high precision positioning system (Endo et al. (1996)). To reject the effects of disturbance, disturbance observer (DOB) was proposed in Ohishi et al. (1983). In ideal disturbance observer configuration as shown in Fig. 1, nominal plant inversion (P_n^{-1}) is utilized to reproduce plant (P_r) input ($u_p = d + u$) and the estimated disturbance ($\hat{d} = \hat{u}_p - u$) is fed back to compensate disturbance (d) influences. In practical applications, low pass filter (Q filter) is necessary to guarantee the causality of system and high bandwidth of the said filter is desired to ensure good disturbance rejection performance.

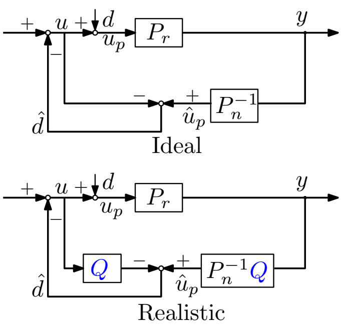

Fig. 1. Block diagram of ideal and realistic disturbance observers

However, the bandwidth of Q filter is limited by unmodeled plant dynamics and noises (Chen et al. (2010), Wang et al. (2004), Choi et al. (2003)). Moreover, in case of a non-minimum phase plant, whose inversion is unstable, internal instability and sensitivity function limitation due to unstable zeros set additional limitations for Q filter design (Sariyildiz et al. (2013), Sariyildiz et al. (2014), and Chen et al. (2004)).

Previous research on Q filter design employed parametric model (transfer function or state space representation) to represent real plant. The fitting process from frequency response data (FRD) to parametric model introduces unmolded plant dynamics which adds the conservatism in shaping Q filter response. To mitigate the influences of unmolded plant dynamics, the direct utilization of FRD information in shaping Q filter response is necessary to be investigated.

Previous frequency response data-based studies mainly focused on designing linearly parameterized fixed order feedback controller while optimizing specifications of control system, such as integrator gain, etc (Karimi et al. (2010), Hast et al. (2013), Nakamura et al. (2016), Galdos et al. (2010)). In regard to aforementioned works, we integrated the frequency response data-based method into DOB optimization design. Second order Q filter design has been investigated in our previous study (Wang et al. (2019)) while this paper focused on arbitrary order Q filter design in which the stability of high order Q filter should be maintained during optimization process.

(1) Systematic method of designing Q filter by FRD is derived. The parameters of Q filter are properly tuned to maximize the bandwidth of DOB and provide satisfactory disturbance attenuation performance.
(2) General derivation process from non-convex constraints to convex constraints in DOB design has been developed. Iterative convex optimization process is established to solve the problem.
(3) No limitations on nominal plant or the Q filter order is required in the proposal.

⋆ The work presented in this paper is supported by JSPS KAKENHI Grant Number 18H05902 and the Telecommunications Advancement Foundation.

The outline of the paper is as follows: In section 2, necessary mathematical preliminaries is provided. Problem formulation is developed in Section 3 in which non-convex constraints are derived. The mathematical transformation process from non-convex constraints to convex constraints is shown in Section 4. Based on the proposal, case study results are shown in Section 5. This paper ends by presenting concluding remarks in Section 6.

2. PRELIMINARIES

A convex optimization problem is one in which the objective and constraint functions are convex, which means they satisfy the inequality:

$$f(\alpha x + \beta y) \leq \alpha f(x) + \beta f(y). \tag{1}$$

for all $x, y \in R^n$ and all $\alpha, \beta \in R^n$ with $\alpha + \beta = 1, \alpha \geq 0, \beta \geq 0$ (Boyd et al. (2004)).

A Linear Matrix Inequality (LMI) has the following form

$$F(x) = F_0 + \sum_{i=1}^{m} x_i F_i > 0, \tag{2}$$

in which $x \in R^m$ is the variable and the symmetric matrices $F_i = F_i^T \in R^{n\times n}$, $i = 0, ..., m$ are given (Boyd et al. (1994)).

Schur Complement (Boyd et al. (1994)) will be used throughout the paper which is introduced as follows.

$$\begin{bmatrix} Q(x) & S(x) \\ (S(x))^T & R(x) \end{bmatrix} > 0, \tag{3}$$

where $Q(x) = Q(x)^T, R(x) = R(x)^T$ and $S(x)$ depends affinely on x, is equivalent to

$$Q(x) > 0, R(x) - S(x)Q(x)^{-1}S(x)^T > 0. \tag{4}$$

Beside these, linear approximation is extensively employed. The basic concept is to estimate the value of a function, $f(x)$, near a point $x_0 = [x_{0(1)}, x_{0(2)}, ..., x_{0(n)}]^T$, using the following formula.

$$f(x) \approx f(x_0) + \nabla f(x_0)(x - x_0). \tag{5}$$

in which ∇ denotes vector differential operator and $\nabla f(x_0) = \left[\dfrac{\partial f(x_0)}{\partial x_{0(1)}}, \dfrac{\partial f(x_0)}{\partial x_{0(2)}}, ..., \dfrac{\partial f(x_0)}{\partial x_{0(n)}}\right]$.

Additionally, $|A|$ denotes the magnitude of A and $j\omega_k$ means sequential frequency points in which j is the imaginary unit while ω_k represents for frequency ([rad/s]) and k means index.

3. PROBLEM FORMULATION

In the disturbance observer control system as shown in Fig. 2, P_r and P_n denote real plant and nominal plant, defined by FRD and transfer function, respectively. Q represents the to-be-designed low pass filter. $d, \hat{d}, u_a, y$ are external disturbance input, estimated disturbance, control input and output, respectively.

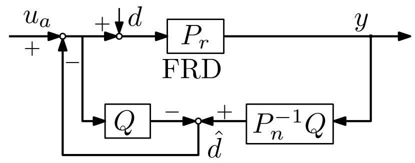

Fig. 2. Block diagram of disturbance observer system

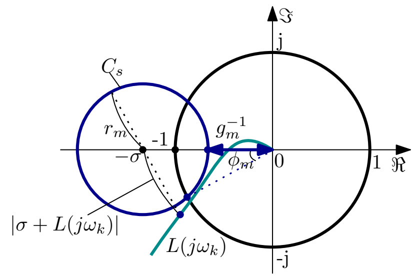

Fig. 3. Circle condition description for prospective Nyquist plot

In this paper, Q is selected as follows in which $a \triangleq [a_1, a_2, ..., a_n]^T$ is the parameter vector to be decided and the order n is selected by designer.

$$Q = \frac{1}{a_n s^n + ... + a_2 s^2 + a_1 s + 1} \triangleq \frac{Q_N}{Q_D}, \tag{6}$$

the following equations are obtained for Fig. 2.

$$\begin{aligned} L &= P_n^{-1} Q(1-Q)^{-1} P_r(j\omega_k) \\ &= \frac{P_r(j\omega_k) P_n^{-1}}{(a_n s^n + ... + a_2 s^2 + a_1 s)} \triangleq \frac{N}{D}, \end{aligned} \tag{7a}$$

$$S = \frac{1}{1 + (1-Q)^{-1} Q P_n^{-1} P_r(j\omega_k)} \triangleq \frac{D}{D+N}, \tag{7b}$$

$$\frac{y}{d} = \frac{P_r(j\omega_k)}{1 + (1-Q)^{-1} Q P_n^{-1} P_r(j\omega_k)} = S P_r(j\omega_k), \tag{7c}$$

$$\frac{\hat{d}}{d} = \frac{(1-Q)^{-1} Q P_n^{-1} P_r(j\omega_k)}{1 + (1-Q)^{-1} Q P_n^{-1} P_r(j\omega_k)} = 1 - S = T, \tag{7d}$$

in which $N = P_r(j\omega_k)P_n^{-1}, D = a_n s^n + ... + a_2 s^2 + a_1 s$ and L, S, T represent the open loop function, sensitivity function and complementary sensitivity function, respectively.

Several constraints are designed to obtain satisfactory disturbance rejection performance. Firstly, the circle condition (Nakamura et al. (2016)) which is shown in Fig. 3 should be met to guarantee the desired gain margin g_m and phase margin ϕ_m. The circle condition is represented by using the following mathematical inequality.

$$|\sigma + L(j\omega_k)| - r_m \geq 0, \tag{8}$$

in which L is the open loop function while center point $(-\sigma, 0)$ and radius r_m of circle C_s are calculated based on the following equations.

$$\sigma = \frac{g_m^2 - 1}{2g_m(g_m \cos\phi_m - 1)}, \tag{9a}$$

$$r_m = \frac{(g_m - 1)^2 + 2g_m(1 - \cos\phi_m)}{2g_m(g_m \cos\phi_m - 1)}. \tag{9b}$$

Secondly, selecting weighting function W_p and W_m as mentioned in (10a) and (10b) for S and T respectively, the constraints for sensitivity function and complementary sensitivity function are established as shown in Fig.

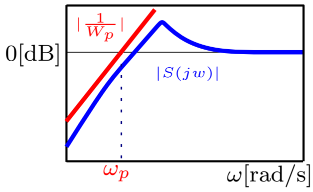

Fig. 4. Figure of constraint for sensitivity function

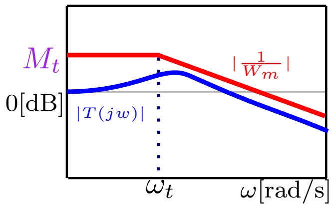

Fig. 5. Figure of constraint for complementary sensitivity function

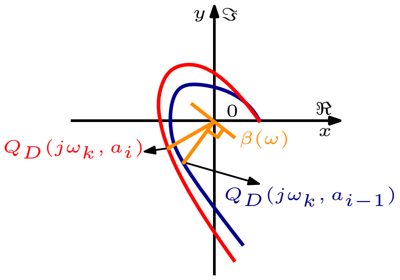

Fig. 6. Explanation of Q filter stability constraint

4 and Fig. 5. ω_p is selected as the optimization objective. ω_t together with $a = [a_1, a_2, ...a_n]^T$ are optimization variables. When the optimal point $\omega_{p(opt)}$ is found, $a = [a_1, a_2, ..., a_n]^T$ is obtained simultaneously. These two constraints are common in conventional $\mathcal{H}_\infty$ theory but obtainable Q is of high order whereas Q has fixed form in this paper.

$$W_p = \frac{\omega_p}{s}, |W_p S| \le 1, \tag{10a}$$
$$W_m = \frac{s + \omega_t}{1.25\omega_t}, \ |W_m T| \le 1, (M_t = 1.25). \tag{10b}$$

Thirdly, the stability of Q filter is guaranteed when the encirclements of the origin by vector loci Q_D and by initial stable Q filter denominator $Q_{D(init)}$ are the same during the optimization process (Shinoda et al. (2016)). The mathematical interpretation is given as (12f) and the meaning of it is $Q_D(j\omega_k, a_i)$ (current value) and $Q_D(j\omega_k, a_{i-1})$ (previous iteration value) are on the same side of the normal line of vector $\overrightarrow{OQ_D}(j\omega_k, a_{i-1})$ at all frequency points as shown in Fig. 6.

$$\begin{aligned} &\Re(Q_D(j\omega_k, a_{i-1}))\Re(Q_D(j\omega_k), a_i) \\ &+ \Im(Q_D(j\omega_k, a_{i-1}))\Im(Q_D(j\omega_k, a_i)) \\ &= \Re(Q_D(j\omega_k, a_{i-1}))Q_D(j\omega_k, a_i)) \ge 0. \end{aligned} \tag{11}$$

In summary, the Q filter design is formulated into the following optimization problem.

$$\underset{a_1, a_2, \cdots, a_n, \omega_t}{\text{Maximize}} \quad \omega_p \tag{12a}$$
$$\text{Subject to} \quad 0 < a_1, a_2, \cdots, a_n, 0 < \omega_p < \omega_t, \tag{12b}$$
$$|L(j\omega_k) + \sigma| \ge r_m, \tag{12c}$$
$$|W_p(j\omega_k, \omega_p)S(j\omega_k)| \le 1, \tag{12d}$$
$$|W_m(j\omega_k, \omega_t)T(j\omega_k)| \le 1, \tag{12e}$$
$$\Re(Q_D(j\omega_k, a_{i-1})Q_D(j\omega_k, a_i)) \ge 0. \tag{12f}$$

4. CONVEX CONSTRAINTS DERIVATION

In this section, the above-listed non-convex constraints are all transformed into linear functions or LMI form of variables $\omega_p, \omega_t, a = [a_1, a_2, \cdots, a_n]^T$. The derived constraints are sufficient condition of original constraints which implies that if the newly-obtained constraints are satisfied, the original constraints hold undoubtedly.

4.1 Constraint in (12c)

In this subsection, (12c) is converted to convex constraint in following way.

$$\begin{aligned} &|L(j\omega_k, a_i) + \sigma| - r_m = \left|\frac{N(j\omega_k)}{D(j\omega_k, a_i)} + \sigma\right| - r_m \ge 0, \\ &\Leftrightarrow |N(j\omega_k) + D(j\omega_k, a_i)\sigma| \ge r_m |D(j\omega_k, a_i)|, \\ &\triangleq F(j\omega_k, a_i) \ge r_m |D(j\omega_k, a_i)|, \\ &\Leftarrow \Psi \ge r_m |D(j\omega_k, a_i)|. \end{aligned} \tag{13}$$

where

$$\begin{aligned} &\Psi = F(j\omega_k, a_{i-1}) + \nabla F(j\omega_k, a_{i-1})(a_i - a_{i-1}), \\ &\nabla F(j\omega_k, a_{i-1}) = \begin{bmatrix} \dfrac{\partial(|N(j\omega_k) + D(j\omega_k, a_{i-1})\sigma|)}{\partial a_{1(i-1)}} \\ \vdots \\ \dfrac{\partial(|N(j\omega_k) + D(j\omega_k, a_{i-1})\sigma|)}{\partial a_{n(i-1)}} \end{bmatrix}^T. \end{aligned} \tag{14}$$

4.2 Constraint in (12d)

For the sensitivity function constraint, the following method is used to obtain LMI form.

$$\begin{aligned} &\left|W_p(j\omega_k, \omega_{p(i)})S(j\omega_k, a_i)\right| \le 1 \\ &\Leftrightarrow \left|\frac{\omega_{p(i)}}{j\omega_k} D(j\omega_k, a_i)\right| \le |D(j\omega_k, a_i) + N(j\omega_k)|. \end{aligned} \tag{15}$$

Squaring the both sides of (15) and turning this inequality into matrix inequality form by using Schur Complement.

$$\begin{aligned} &\left|\frac{\omega_{p(i)}}{j\omega_k}\right|^2 |D(j\omega_k, a_i)|^2 \le |D(j\omega_k, a_i) + N(j\omega_k)|^2, \\ &\Leftrightarrow \begin{bmatrix} \left|\dfrac{\omega_k}{\omega_{p(i)}}\right|^2 & D(j\omega_k, a_i) \\ (D(j\omega_k, a_i))^* & |D(j\omega_k, a_i) + N(j\omega_k)|^2 \end{bmatrix} \\ &\triangleq \begin{bmatrix} S_{11} & S_{12} \\ (S_{12})^* & S_{22} \end{bmatrix} \ge 0. \end{aligned} \tag{16}$$

To obtain the sufficient condition of original constraint, the lower bound of S_{11} and S_{22} are required. For $S_{11} = \frac{(\omega_k)^2}{\omega_{p(i)}^2}$, the lower bound of $\omega_{p(i)}^{-2}$ is obtained by using the following technique (Shinoda et al. (2016)).

$$\begin{aligned}
&(\omega_{p(i)}^{-2} - \omega_{p(i-1)}^{-2})(\omega_{p(i)}^{-2} - \omega_{p(i-1)}^{-2}) \geq 0, \\
&\Leftrightarrow \omega_{p(i)}^{-4} \geq 2\omega_{p(i-1)}^{-2}\omega_{p(i)}^{-2} - \omega_{p(i-1)}^{-4}, \\
&\Leftrightarrow \omega_{p(i)}^{-2} \geq 2\omega_{p(i-1)}^{-2} - \omega_{p(i-1)}^{-4} w_{p(i)}^{2} \geq \phi_{1(i)} > 0.
\end{aligned} \tag{17}$$

in which $\phi_{1(i)}$ is newly-introduced variable and constraints for it can be expressed in the following form:

$$\begin{bmatrix} 2\omega_{p(i-1)}^2 - \phi_1\omega_{p(i-1)}^4 & \omega_{p(i)} \\ \omega_{pi} & 1 \end{bmatrix} > 0, \phi_{1(i)} > 0. \tag{18}$$

In conclusion, $S_{11} = \frac{\omega_k^2}{\omega_{p(i)}^2} \geq \omega_k^2\phi_{1(i)}$.

As for S_{22}, the linear approximation is employed.

$$\begin{aligned}
&S_{22} = |D(j\omega_k, a_i) + N(j\omega_k)|^2 \triangleq (M(j\omega_k, a_i))^2 \\
&\geq (M(j\omega_k, a_{i-1}))^2 + \nabla(M(j\omega_k, a_{i-1}))^2(a_i - a_{i-1}) = \Phi,
\end{aligned} \tag{19}$$

in which

$$\nabla(M(j\omega_k, a_{i-1}))^2 = \begin{bmatrix} \dfrac{\partial(|N(j\omega_k) + D(j\omega_k, a_{i-1})|^2)}{\partial a_{1(i-1)}} \\ \vdots \\ \dfrac{\partial(|N(j\omega_k) + D(j\omega_k, a_{i-1})|^2)}{\partial a_{n(i-1)}} \end{bmatrix}^T \tag{20}$$

In summary, the original nonlinear constraint (12d) is transformed into the following LMIs by combining (16), (18) and (19).

$$\begin{bmatrix} \omega_k^2\phi_{1(i)} & D(j\omega_k, a_i) \\ (D(j\omega_k, a_i))^* & \Phi \end{bmatrix} \geq 0, \ \phi_{1(i)} > 0, \tag{21a}$$

$$\begin{bmatrix} 2\omega_{p(i-1)}^2 - \phi_{1(i)}\omega_{p(i-1)}^4 & \omega_{p(i)} \\ \omega_{p(i)} & 1 \end{bmatrix} > 0. \tag{21b}$$

4.3 Constraint in (12e)

Following the similar process as used in dealing with (12d), the complementary sensitivity function constraint (12e) is changed into the following form.

$$\begin{aligned}
&\left|W_m(j\omega_k, \omega_{t(i)})T(j\omega_k, a_i)\right| \leq 1, \\
&\Leftrightarrow \left|\frac{s + \omega_{t(i)}}{1.25\omega_{t(i)}}\right|^2 \leq \left|\frac{D(j\omega_k, a_i) + N(j\omega_k)}{N(j\omega_k)}\right|^2, \\
&\Leftrightarrow \begin{bmatrix} \omega_{t(i)}^2 & \dfrac{|N(j\omega_k)|(s + \omega_{t(i)})}{1.25} \\ \dfrac{|N(j\omega_k)|(s + \omega_{t(i)})^*}{1.25} & |D(j\omega_k, a_i) + N(j\omega_k)|^2 \end{bmatrix} \geq 0, \\
&\triangleq \begin{bmatrix} T_{11} & T_{12} \\ (T_{12})^* & T_{22} \end{bmatrix} \geq 0.
\end{aligned} \tag{22}$$

As before, T_{11} and T_{22} needs transformation. Since $T_{22} = S_{22}$, this part is omitted due to the repetition. For T_{11},

$$\omega_{t(i)}^2 \geq 2\omega_{t(i-1)}\omega_{t(i)} - \omega_{t(i-1)}^2. \tag{23}$$

By combining (19), (22) and (23), the original non-convex constraint is changed into

$$\begin{bmatrix} 2\omega_{t(i-1)}\omega_{t(i)} - \omega_{t(i-1)}^2 & \dfrac{|N(j\omega_k)|(s + \omega_{t(i)})}{1.25} \\ \dfrac{|N(j\omega_k)|(s + \omega_{t(i)})^*}{1.25} & \Phi \end{bmatrix} \geq 0. \tag{24}$$

4.4 Problem Reformulation

After finishing all the process mentioned above, the original problem is reformulated as follows.

Maximize $\quad \omega_p$

Subject to

$$0 < a_{1(i)}, \cdots, a_{n(i)}, \tag{25a}$$

$$0 < w_{p(i)} < w_{t(i)}, 0 < \phi_{1(i)}, \tag{25b}$$

$$\Psi - r_m D(j\omega_k, a_i) \geq 0, \tag{25c}$$

$$\Re(Q_D(j\omega_k, a_{i-1})Q_D(j\omega_k, a_i)) \geq 0, \tag{25d}$$

$$\begin{bmatrix} \omega_k^2\phi_{1(i)} & D(j\omega_k, a_i) \\ (D(j\omega_k, a_i))^* & \Phi \end{bmatrix} \geq 0, \tag{25e}$$

$$\begin{bmatrix} 2\omega_{p(i-1)}^2 - \phi_{1(i)}\omega_{p(i-1)}^4 & \omega_{p(i)} \\ \omega_{p(i)} & 1 \end{bmatrix} \geq 0, \tag{25f}$$

$$\begin{bmatrix} 2\omega_{t(i-1)}\omega_{t(i)} - \omega_{t(i-1)}^2 & \frac{|N(j\omega_k)|(j\omega_k + \omega_{t(i)})}{1.25} \\ \frac{|N(j\omega_k)|(j\omega_k + \omega_{t(i)})^*}{1.25} & \Phi \end{bmatrix} \geq 0. \tag{25g}$$

The new optimization problem is a convex optimization problem and can be solved by commercial solvers.

5. CASE STUDY

5.1 Plant and simulation condition

The simplified model of simulation plant is shown in Fig. 7. The linear motor (actuator) provides actuation force (input, F) and moves table towards predefined position. The position of table (output or control target x) is recorded by table side linear encoder. Input disturbances are taken into account, e.g. friction of linear motor side.

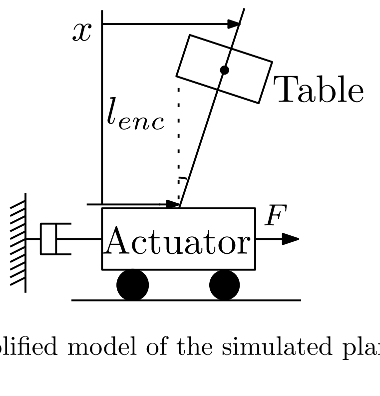

Fig. 7. Simplified model of the simulated plant

The real plant and nominal plant are represented by FRD ($P_r(j\omega_k)$) and transfer function (P_n), respectively.

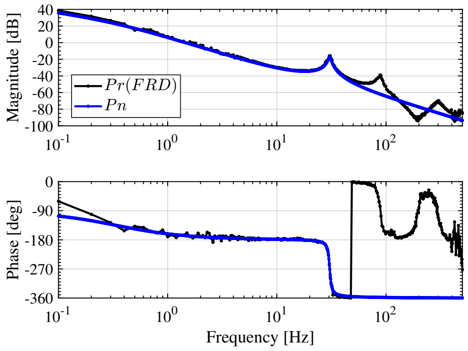

Fig. 8. Bode plots of plant FRD (P_r (FRD)) and nominal plant (P_n)

Nominal plant P_n is selected as a fourth order non-minimum phase one as represented in (26). Bode plots of $P_r(FRD)$ and P_n are shown in Fig. 8.

$$P_n = \frac{-206.68(s-125.6)(s+120)}{s(s+2.101)(s^2+10.89s+3.665\times10^4)}. \tag{26}$$

Since the inversion of nominal plant is unstable, zero phase error approximation (Tomizuka (1987)) of nominal plant inversion is employed and Q is selected as a fourth order filter to guarantee the causality of system.

$$\bar{P}_n^{-1} = \frac{s(s+2.101)(s+125.6)(s^2+10.89s+3.665\times10^4)}{3.2614\times10^6(s+120)}, \tag{27a}$$

$$Q = \frac{1}{a_4s^4+a_3s^3+a_2s^2+a_1s+1}. \tag{27b}$$

The corresponding L, S and T are obtained.

$$L = \frac{P_r(j\omega_k)\bar{P}_n^{-1}}{a_4s^4+a_3s^3+a_2s^2+a_1s}, \tag{28a}$$

$$S = \frac{a_4s^4+a_3s^3+a_2s^2+a_1s}{a_4s^4+a_3s^3+a_2s^2+a_1s+P_r(j\omega_k)\bar{P}_n^{-1}}, \tag{28b}$$

$$T = \frac{P_r(j\omega)\bar{P}_n^{-1}}{a_4s^4+a_3s^3+a_2s^2+a_1s+P_r(j\omega_k)\bar{P}_n^{-1}}. \tag{28c}$$

During the simulation, desired gain margin and phase margin are 6dB and 30°. According to (9a) and (9b), $\sigma = 1.03, r_m = 0.525$.

The initial condition for optimization is $a_1 = 0.0838, a_2 = 1.76\times10^{-3}, a_3 = 5.668\times10^{-7}, a_4 = 3.343\times10^{-9}, \omega_p = 9.9$ [rad/s]. The criterion for selecting initial condition is to satisfy the constraints. The convex constraints are established using our proposed method, followed by optimization of the said problem using off the shelf toolboxes, Yalmip (Löfberg (2004)) and Mosek (Mosek (2019)) in Matlab.

5.2 Simulation result

After optimization, $\omega_{p(opt)} = 41.46$ [rad/s] (6.60 [Hz]) and $a_1 = 0.019, a_2 = 2.99\times10^{-4}, a_3 = 3.62\times10^{-7}, a_4 = 1.169\times10^{-9}$. Tuned Q filter's bandwidth is 11.86 [Hz]. The resultant Nyquist plots of open loop function, before and after optimization are shown in Fig. 9. Dashed black line represents unit circle and dotted black line is a circle whose center is located at $(-\sigma,0)$, i.e. $(-1.03,\ 0)$ and the

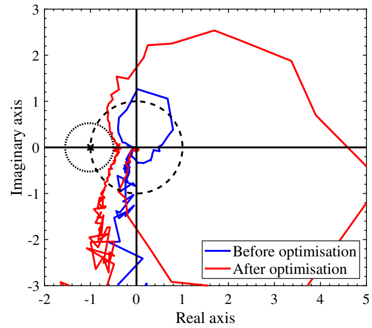

Fig. 9. Nyquist plots of before and after optimization

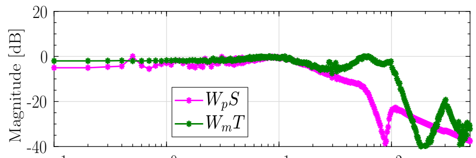

Fig. 10. Magnitude plots of W_pS and W_mT

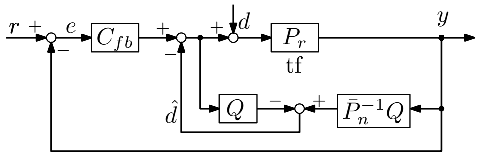

Fig. 11. Block diagram of disturbance compensation based on DOB

radius (r_m) is 0.525. The stability margin constraint, (12c), holds successfully as the Nyquist plot has no intersection with the dotted circle. With the stability margin constraint satisfied, the peak value of sensitivity function is limited because the closest distance from Nyquist plot to critical point $(-1, 0)$ is the inverse of the peak value of the sensitivity function. Finally, proposed optimization method forces the Nyquist plot to be tangent to the dotted circle which implies that the bandwidth of open loop function is maximized under the limitation of constraints. The constraints for S and T are satisfied as $|W_pS|$ and $|W_mT|$ are always under 0 dB in Fig. 10.

5.3 Disturbance Rejection Performance

Simulations have been conducted to test the disturbance rejection performance of above-designed Q filter by using Fig. 11. P_r is a well-identified 8th order transfer function (tf) which is shown with the feedback controller C_{fb} as follows.

$$P_r = \frac{164.38(s+1089)(s-878)(s-125.6)}{s(s+2.101)(s^2+10.89s+3.665\times10^4)} \times \frac{(s+120)(s^2+185.5s+1.447\times10^6)}{(s^2+45.4s+3.139\times10^5)(s^2+262.2s+3.507\times10^6)}, \tag{29}$$

$$C_{fb} = 1.36 + \frac{3.64}{s} + \frac{0.261s}{0.0249s+1}. \tag{30}$$

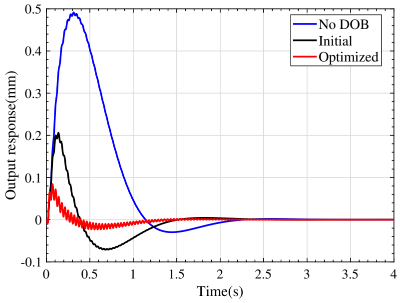

Fig. 12. Disturbance rejection performance comparison result

By making reference input as zero and injecting unit step disturbance to the system, three different output responses are obtained for comparison.

(1) Only feedback controller C_{fb} works in the system.
(2) Selected initial disturbance observer plus feedback controller C_{fb} work in the system together.
(3) Optimized disturbance observer plus feedback controller C_{fb} work in the system together.

The proposed Q filter design outperforms the initial design and the disturbance rejection performance has been improved as illustrated in Fig. 12. The maximum deviation from reference position has been decreased by 59.1% as compared to initial DOB and by 82.8% as compared to feedback controller only case.

6. CONCLUSION

This paper has proposed a general design method for maximizing bandwidth of disturbance observer directly based on frequency response data. Moreover, all the non-convex constraints have been transformed into convex form which are solved by convex optimization method. The numerical case study validated the proposed method.

ACKNOWLEDGEMENTS

The student author is grateful to China Scholarship Council (CSC) for supporting her. The authors cordially thank Professor Hiroshi Fujimoto (The University of Tokyo) for providing the frequency response data.

REFERENCES

S. Endo, H. Kobayashi, C. J. Kempf, S. Kobayashi, M. Tomizuka, and Y. Hori. Robust digital tracking controller design for high-speed positioning systems. *Control Engineering Practice*, volume 4, pages 527–536, 1996.

K. Ohishi, K. Ohnishi, and K. Miyachi. Torque-speed regulation of DC motor based on load torque estimation method. *International Power Electronics Conference*, pages 1209–1218, 1983.

X. Chen and M. Tomizuka. Optimal plant shaping for high bandwidth disturbance rejection in discrete disturbance observers. *Proceedings of the American Control Conference*, pages 2641–2646, 2010.

C. C. Wang and M. Tomizuka. Design of robustly stable disturbance observers based on closed loop consideration using H_∞ optimization and its applications to motion control systems. *Proceedings of the American Control Conference*, pages 3764–3769, 2004.

Y. Choi, K. Yang, W. K. Chung, H. R. Kim and I. H. Suh. On the robustness and performance of disturbance observers for second-order systems. *IEEE Transactions on Automatic Control*, volume 48, pages 315–320, 2003.

E. Sariyildiz and K. Ohnishi. A new solution for the robust control problem of non-minimum phase systems using disturbance observer. *IEEE International Conference on Mechatronics*, pages 46–51, 2013.

E. Sariyildiz and K. Ohnishi. A Guide to design disturbance observer. *Journal of Dynamic Systems, Measurement, and Control*, volume 136, 2014.

X. Chen, G. Zhai, and T. Fukuda. An approximate inverse system for nonminimum-phase systems and its application to disturbance observer. *Systems & Control Letters*, volume 52, pages 193-207, 2004.

A. Karimi and G. Galdos. Fixed-order H_∞ controller design for nonparametric models by convex optimization. *Automatica*, volume 46, pages 1388–1394, 2010.

M. Hast, K. J. Åström, B. Bernhardsson, and S. Boyd. PID design by convex-concave optimization. *Proceedings of the European Control Conference*, pages 4460–4465, 2013.

K. Nakamura, K. Yubai, D. Yashiro, and S. Komada. Controller design method achieving maximization of control bandwidth by using Nyquist diagram. *Proceedings of the International Automatic Control Conference*, pages 35–40, 2016.

G. Galdos, A. Karimi, and R. Longchamp. H_∞ controller design for spectral MIMO models by convex optimization. *Journal of Process Control*, volume 20, pages 1175–1182, 2010.

X. Wang, W. Ohnishi and T. Koseki. Frequency response data based disturbance observer design applicable to non-minimum phase systems. *Proceedings of the Annual Conference of the Society of Instrument and Control Engineers of Japan*, pages 358–363, 2019.

S. Boyd and L. Vandenberghe. Convex Optimization. *Cambridge University Press*, 2004.

S. Boyd, L. El Ghaoui, E. Feron, and V. Balakrishnan. Linear Matrix Inequalities in System and Control Theory. *Society for Industrial and Applied Mathematics*, 1994.

S. Shinoda, K. Yubai, D. Yashiro, J. Hirai. Fully parameterized multivariable controller design minimizing closed-loop interaction by iterative LMI optimization. *IEEJ international workshop on Sensing, Actuation, and motion Control*, TT3-6, 2016.

M. Tomizuka. Zero phase error tracking algorithm for digital control. *Journal of Dynamic Systems, Measurement, and Control*, volume 109, pages 65–68, 1987.

J. Löfberg. YALMIP : a toolbox for modeling and optimization in MATLAB. *IEEE International Conference on Robotics and Automation*, pages 284–289, 2004.

MOSEK ApS. MOSEK optimization toolbox for MATLAB manual. 2019.